Environmental Science
Water Research & Technology

ROYAL SOCIETY OF CHEMISTRY

PAPER

View Article Online
View Journal | View Issue

Cite this: *Environ. Sci.: Water Res. Technol.*, 2025, **11**, 3083

Examining the growth and mobilization behavior of early-stage biofilms in a controlled, pilot scale PVC drinking water system laboratory

Artur Sass Braga, * Yves Filion and Benjamin Anderson

Received 14th July 2025,
Accepted 14th October 2025

DOI: 10.1039/d5ew00654f

rsc.li/es-water

The aim of this paper was to examine the growth and mobilization behavior of early-stage biofilms in a pilot scale, controlled PVC drinking water system. An alternative method for biofilm growth used a concentrated solution of microorganisms sourced in tap water to inoculate the pipe system and allowed biofilms to be formed over a 28-day period. Biofilm development was also assisted with nutrient addition and disinfection depletion from the experimental system water. The pipe loop was then flushed to mobilize these biofilms. The growth and mobilization of the biofilms were assessed with molecular and fluorescence microscopy analysis of bulk water samples and removable pipe wall samples. Results showed that: (1) biofilms followed a rapid growth period on the pipe wall between 0 and 14 days, and 21 and 28 days; (2) biofilm growth was apparently halted between 14 and 21 days, likely because of a shift in bacterial community composition; (3) biofilms were observed to preferentially accumulate at the invert pipe position along the full longitudinal direction of the pipe but rapidly decreased for the springline and obvert circumferential positions of the pipe; (4) a flushing flow of 6.5 L s^{-1} (1.2 Pa) was not able to fully remove the biofilms from the pipe wall; (5) biofilms were observed to form in clusters on the pipe wall which remained fully attached to the pipe wall even after flushing. Biofilms investigated here were likely impacted by the alternative growth method, but their physical structure still resembles biofilms from operational DWDSs. The research findings add to the emerging knowledge concerning the growth and mobilization of biofilms in drinking water systems. In addition, the alternative method to investigate biofilms is highly reproducible and can facilitate future studies in the field.

Water impact

Biofilms are pervasive in drinking water systems and can contribute to the accumulation of contaminants that affect water quality. This study revealed important characteristics of early-stage biofilms grown in PVC pipe mains, as well as the impact of hydraulic forces on their accumulation and mobilization from pipe walls. These results add to the emerging body of knowledge on drinking water biofilms and will support water utilities in managing biofilms within operational networks.

Introduction

Biofilms are pervasive in drinking water distribution systems (DWDSs) and are often linked to water quality problems in these systems. In the context of DWDSs, biofilms are communities of active microorganisms that are attached to the inner surface of drinking water pipes.[1] The microorganisms in biofilms often produce extracellular polymeric substances (EPSs) made up of macromolecules such as proteins, humic acid, polysaccharides, and nucleic acid to give structure and impart strength to the biofilm matrix and enable diverse functions within the biofilm environment.[1] EPSs also help biofilms resist shearing forces and protect microorganisms from disinfectants in drinking water pipes.

The growth and evolution of biofilms follows a number of steps. Biofilms are typically initiated by colonies of microorganisms that are well adapted to attach to solid surfaces. These microbial colonizers then grow into macroscopic structures with thicknesses ranging from a few microns to several millimeters that cover internal surfaces of a drinking water pipe.[2,3] The production of EPSs by bacterial species such as *Pseudomonas aeruginosa* and *Staphylococcus aureus* facilitates the attachment of additional microorganisms which allows the biofilm to grow and enhances its overall functioning. Over time, the

Department of Civil Engineering, Queen's University, Ellis Hall, 58 University Ave, Kingston, Ontario, K7L 3N9, Canada. E-mail: asb9@queensu.ca, yves.filion@queensu.ca, ben.anderson@queensu.ca

microorganisms inside a biofilm tend to establish a high level of cooperation between each other and take advantage of available inorganic matter[4,5] to make the biofilm adaptable to the prevailing environmental conditions[6,7] inside the drinking water pipe.

Biofilms are an important consideration in the management of drinking water systems because of their established links to poor drinking water quality. First, biofilms can harbor pathogens that can cause gastroenteric disease in humans if ingested.[8] Second, biofilms can contribute to the biocorrosion of iron pipes.[9,10] Third, biofilms are known to be able to capture and release particulate and dissolved metals[11,12] such as iron and manganese that can cause discoloration events and trigger customer complaints.[13,14] For these reasons, gaining an understanding of how biofilms evolve and grow in both time and space is necessary to devise strategies to control and eliminate them from drinking water pipes.

Investigating biofilms in DWDSs is challenging due to their specificity, spatial and temporal heterogeneity, and the inaccessibility of the buried infrastructure.[15] As a result, researchers have developed a variety of experimental designs to study biofilms under controlled conditions.[16,17] Benchtop reactors (*e.g.*, flow cells, annular reactors, and CDC reactors) have become popular due to their simple operation and ability to partially replicate DWDS conditions. Typical experiments involve continuously feeding reactors with local drinking water over extended periods (4–132 weeks) to grow biofilms on retrievable surfaces (*e.g.*, coupons, slits, or squares) for analysis.[16–21] Sample materials are selected to match the composition of DWDS pipes, such as cast iron, polyvinyl chloride (PVC), high density polyethylene (HDPE), copper, or stainless steel. Additionally, various parameters, such as temperature, flow rate, hydraulic retention time, water age, turbulence, and wall shear stress, can be controlled to tailor experiments to specific research objectives.[22,23] Despite these advantages, benchtop reactors have scale limitations that result in different fluid dynamics compared to full-scale pipe systems. Moreover, their sample configurations do not replicate the velocity profiles found in actual pipe flows. Consequently, questions remain about how well biofilms grown in benchtop reactors resemble those in real DWDS environments.

To address these concerns, alternative experiments using pilot systems have been developed.[24–31] These include parallel pipe section rigs and looped pipe rigs, which may be connected to the water supply or operate independently using dedicated pumps and water tanks. Most pilot systems in the literature use small-diameter pipes and are designed to study premise plumbing rather than large-scale distribution networks.[18,28,30,32] But a number of researchers have also used pilot scale distribution pipe laboratories to carry out these investigations. Researchers at the University of Sheffield in the UK have used three pilot scale HDPE pipe loops to examine biofilms and discoloration issues while replicating DWDS hydraulics and water quality.[24–27] Researchers at Queen's University in Kingston, Canada have used two pilot scale PVC pipe loops to examine particle accumulation and mobilization in the presence and absence of biofilms.[33,34] More recently, researchers at Ghent University in Belgium have developed three PVC pipe loops (DN 80 mm) to examine biofilms and discolouration issues in drinking water.[35,36]

In addition to these experimental setups, the methods used to assess the biofilms in DWDSs are diverse and non-standardized in the research literature.[27] Cell counting achieved *via* microscopy or flow cytometry is the most commonly used method to characterize biofilms,[22,27,29,30,32] even though extracellular polymeric substances (EPSs) are reported to constitute up to 90% of biofilms.[1] Furthermore, studies suggest that biofilms regulate their EPS production in response to environmental conditions,[1] making the EPS-to-cell ratio a highly variable and unreliable proxy.

ATP measurement is another widely used method to characterize biofilms.[23,29,30] While the quantification of ATP provides valuable insights into biofilm activity, it does not necessarily correlate with the total organic matter present in the biofilm. Molecular techniques, such as qPCR that targets bacterial 16S rRNA genes or fungal ITS regions, have also been employed.[27,37,38] These methods have significantly enhanced our understanding of biofilms, especially when combined with DNA sequencing. However, DNA can originate from live or dead cells, EPSs, or entrapped external organic materials, making it difficult to identify sources and correlate DNA content with quantitative estimates of biofilms.

Some studies have also characterized biofilms through microscopy imaging—either by counting clusters of biofilms[39] or using confocal laser scanning microscopy (CLSM) directly on coupons.[21,26] These techniques provide valuable structural insights but have limitations insofar as the quantitative characterization of biofilms is concerned. For instance, microscopy-based volume calculations are prone to inaccuracies, and the absence of density information makes it difficult to convert volume to mass.

The lack of standardized biofilm characterization methods is an existing research gap, particularly when translating experimental findings into practical applications in operational DWDSs.[21,40] Recent research has advanced our understanding of the relationship between biofilms and drinking water quality, including their interactions with disinfectants,[41] the accumulation of contaminants, and the presence of pathogens.[39,42,43] However, limited data are available on the quantitative characterization of biofilms and their growth dynamics within pipe networks.

Research also suggests that biofilms contribute to sediment buildup and discoloration issues in distribution systems.[14] The interaction between biofilms and sediment accumulation on pipe walls is particularly important for managing drinking water quality due to the physical characteristics of biofilm EPSs. EPS materials exhibit strong adhesion to surfaces, are viscoelastic—capable of resisting high shear forces—and are bioengineered to capture resources from the bulk flow.[1,5]

It is hypothesized that biofilm EPSs enhance the attachment of suspended particles from the bulk water onto pipe walls.[44] Conversely, sediment accumulation can create a favorable environment for biofilm development by offering protection from the hydraulic forces of water flow. These synergies between biofilms and sediments are often cited as driving factors behind the buildup of material layers inside DWDSs, and are a primary cause of customer complaints regarding drinking water quality.[44–46]

The high resistance of biofilms to mobilization is also believed to impact pipe cleaning strategies (*e.g.*, flushing),[47] as well as accelerate the reformation of material layers on pipe walls,[41,44] thereby increasing the risk of recurring water quality deterioration events.

A major challenge in investigating the relationship between biofilm EPSs and material accumulation in full-scale systems is the lack of control over biofilm growth conditions and the near impossibility of reproducing experiments due to the multitude of environmental variables influencing biofilm development.

To address this, the present study proposes an alternative experimental method using a pilot-scale facility, designed to facilitate the investigation of biofilm physical characteristics in DWDSs. Developing reliable methods to characterize biofilm growth under diverse DWDS conditions in quantitative terms is essential for effective risk assessment and water quality management.

The aim of this paper is to examine the growth and mobilization behavior of early-stage biofilms in both quantitative and qualitative terms in a pilot scale, controlled PVC drinking water system. The specific objectives are to examine: (1) the growth behavior of biofilms in the longitudinal and circumferential locations of drinking water pipes and (2) the mobilization behavior of the biofilms when subjected to high shear stress during flushing.

Methods

Drinking water distribution laboratory

The drinking water distribution laboratory (DWDL) is located in Kingston, Ontario, Canada and draws its source water from the King St. Water Treatment Facility on the shore of Lake Ontario at the mouth of the St. Lawrence River.[48] The King St. Water Treatment Facility is located 5 km from the DWDL and includes the unit processes of pre-chlorination, screening, coagulation/flocculation, filtration, and post-chlorination. Once the water leaves the discharge works of the King St. treatment plant, sodium hypochlorite is added to the water in a clear well to create a chlorine residual in the Kingston distribution system.[48] The DWDL is connected to the Kingston network *via* a 150 mm cast iron (CI) water service line installed in the 1970s.

The water quality conditions in the Kingston distribution network that supplies the DWDL are indicated in Table 1. The pH is close to neutral and the average water temperature at the discharge works of the King St. treatment plant is approximately 12 °C. Kingston water has a low level of turbidity (<0.2 NTU) and an average free chlorine concentration that ranges between 2.7 mg L^{-1} near the King St. treatment plant and the DWDL and 0.17 mg L^{-1} at the periphery of the network.

The drinking water biofilm growth experiments were carried out in the DWDL. The laboratory is composed of two independent pipe loop systems, each measuring 200 m in length, which are used to simulate the operation of water networks (Fig. 1). The pipe loops are composed of 100 mm diameter Blue Brute PVC pipes from IPEX that are widely used in new water main projects in North America. Pumps convey water to the inlet (bottom of the loop in Fig. 1), and water exits the loop at the outlet (top of the loop in Fig. 1) where it is conveyed to a tank (3.6 m^3) or to a drain, depending on the situation. The hydraulic and water quality conditions in the loops are monitored by means of bulk water sampling ports, removable pipe coupons, and on-line instruments.

The goal of the experiments was to observe the evolution of early-stage biofilms in a drinking water pipe and achieve reproducible biofilms with physical characteristics that partially resemble biofilms in operational DWDSs. Previous studies have shown that the physical structure of the EPSs of biofilms is largely determined by external forces.[5,49–51] Therefore, our main goal here was to enable controlled growth of biofilms under the influence of suitable hydraulic forces that occur in DWDSs. The experiments were composed of two phases: a 28 d biofilm growth phase and a biofilm mobilization phase through flushing. A key difference of these experiments, in contrast to conventional drinking water biofilm studies, was

Table 1 Water quality parameters for the Kingston system and water in pipe loops A and B during the biofilm growth phase

Water quality parameter[a]	Kingston system[c]	Pipe loop A	Pipe loop B
pH	7.20–8.15[d]	7.75	7.92
Water temperature (°C)	12.3[e]	16.7	16.9
Dissolved oxygen (mg L^{-1})[b]	N/A	5.2–10.9	4.9–11.0
Specific conductivity (μS cm^{-1})	303–324[d]	359	312
Turbidity (NTU)	0.056–0.197[e]	0.287	0.342
Chlorine residual (mg L^{-1})	0.17–2.7[d]	~0	~0

[a] Water quality parameters are averages of measurements taken during the 28 d growth period in pipe loops A and B, unless otherwise specified. [b] Dissolved oxygen values reported correspond to average, minimum, and maximum values measured during the 28 d growth period. [c] Source water quality parameters taken from 2023 King Street Water Treatment Plant Annual Report, Utilities Kingston. [d] Measured in the Kingston distribution system. [e] Measured at discharge works of the Kingston King St. WTP.

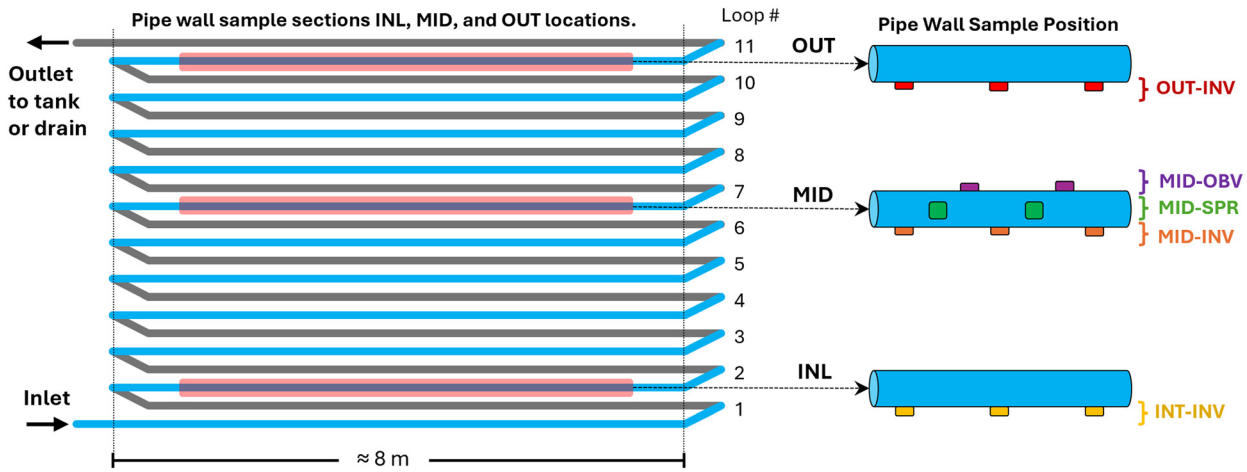

Fig. 1 Location of pipe wall sample sections (INL, MID and OUT) in the pipe loop, and the pipe wall sample positions: 1) at the pipe section INL invert (INL-INV), 2) at the pipe section MID invert (MID-INV), 3) at the pipe section MID springline (MID-SPR), 4) at the pipe section MID obvert (MID OBV), and 5) at the pipe section OUT invert (OUT-INV).

the use of a GAC filter to grow and collect cells and biofilms on the GAC media to then introduce them in the pipe loops to facilitate biofilm growth. At the beginning of the growth phase, a bacterial broth was injected into the pipe loop. Throughout the growth phase, nutrients were continuously added to the pipe loops to encourage the growth of biofilms. After the 28 d growth phase, the pipe loops were flushed with a high flow rate to mobilize the biofilms. The experiment was performed in duplicate using two independent pipe loop systems (loop A and loop B), with the same hydraulic and water quality conditions.

Pre-experimental cleaning and disinfection

Prior to starting the 28 d biofilm growth phase, all wet surfaces in pipe loops A and B were disinfected with a sodium hypochlorite solution at a final free chlorine concentration of 20 mg L^{-1} and a contact time of 24 h. Following this, both pipe loops A and B were flushed at a flow rate of 15 L s^{-1} (1.6 m s^{-1}, 5.6 Pa) with Kingston water, and the flush water was conveyed to a drain. Sodium thiosulfate was introduced into pipe loops A and B to reduce background concentrations of free chlorine to zero in the pipe loops prior to starting the experiment. Water quality conditions in the pipe loops were stabilized in the following 24 h period.

Initial bacterial broth (IBB) and pipe loop inoculation

The starting point of the experiments was to harvest an adequate number of microorganisms to produce drinking water biofilms in the pipe loops. Harvesting biofilm-forming microorganisms from drinking water was intended to accelerate the colonization of clean pipe surfaces and enhance the reproducibility of future experiments. To achieve a consistent inoculum but still maintain its connection with the local drinking water system, a bespoke filtration system was developed to continuously harvest viable microorganisms from the Kingston water. Pinto, Xi and Raskin[52] showed that filtration processes govern the microbiome of DWDSs, therefore being an ideal setup to concentrate a representative community of microorganisms harvested from tap water. This system consisted of a water heater installed in series with two granular activated charcoal (GAC) filters that were connected to a local water tap and operated with a continuous flow rate of 0.5 L min^{-1} for several months. At the intake, the tap water temperature was controlled at 20 °C. The first GAC column was used to strip chlorine from the Kingston water. The second GAC column was used to accumulate viable bacteria present in the Kingston water by providing a substrate onto which bacteria could colonize the high surface area of the charcoal to form biofilms.

The effluent from the second GAC provided a stable output of new colonizer cells. However, due to the low nutrient concentration in the Kingston water, the cell concentration at the GAC effluent was still relatively small (<100 CFU mL^{-1}). To achieve enough microbes to inoculate a pilot scale system, an initial bacterial broth (IBB) was developed with GAC effluent water and nutrient broth. Specifically, 18 L of GAC effluent water was combined with 1.5 L of nutrient broth NutriSelect® Plus No. 3 (concentration of 13 g L^{-1}) and incubated for one week at 16 °C under agitation. Prior to introducing the IBB into the pipe loops, the cell concentration of the IBB was measured in triplicate with flow cytometry and found to be 2.3×10^5 cells per mL. To initiate the experiment, a 2 L volume of IBB was poured into the mouth of each tank connected to the pipe loops. The inoculation of each pipe loop with the IBB made it possible to grow biofilms in the pipe loops.

Biofilm growth phase

Immediately after the pipe loops were inoculated with the IBB, the flow rate was then set to 0.6 L s^{-1} (0.07 m s^{-1}, 0.015 Pa) and held constant until the end of the biofilm growth

period of 28 days. The water was continuously recirculated between the tank and the pipe loop, with a residence time inside the pipe loop of ~50 minutes. This flow rate is representative of the average day flow experiences in local distribution mains of Canadian systems.[34,53] The water temperature was maintained at 16 °C which is typical in Canadian drinking water systems during the summer period.[26,34,54–56] Sterilized nutrient broth NutriSelect® Plus No. 3 was continuously injected into the tanks at an average rate of 1.2 mg L^{-1} per day (3720 mg per day) to promote biofilm growth throughout the 28 d growth period. A total of 105 g of nutrient broth was added to each pipe loop over the 28 d period. At the start of the experiment, dissolved oxygen (DO) was measured to be at or near saturation for the average water temperature of 16 °C. After 2 weeks into the biofilm growth period, DO concentrations reached a near-constant value of 5 mg L^{-1} (Table 1, Fig. S1). This suggests that the system reached a balance between DO consumption from microbial respiration and DO replenishment through diffusion in the tanks. Here, the microorganisms in the biofilms likely experienced some stress because of these low DO concentrations in the second half of the growth period.

Fig. 2 shows the time series plots of non-purgeable organic carbon (NPOC) (Fig. 2a) and total nitrogen (TN) (Fig. 2b) established in pipe loops A and B during the 28 d growth phase. The average concentrations of NPOC and TN were 2.35 mg L^{-1} and 0.78 mg L^{-1} in the bulk water during the 28 d growth period. Generally, the NPOC and TN concentrations were comparable across pipe loops A and B. Fig. 2a and b clearly show a steady increase in NPOC and TN during the 28 d growth phase. This suggests that dissolved carbon and nitrogen likely did not limit the growth of planktonic microorganisms in the bulk water or on the pipe wall.

The assessment of biofilm community composition was beyond the scope of this study. However, the bacterial community composition assessed in preliminary experiments using the GAC and the pipe loop revealed the presence of common bacteria genera found in DWDSs (*e.g.*, Pseudomonas, Acinetobacter, Bacillus, Sediminibacterium, Legionella, Bosea, and Rhodobacter). The relative abundance plot of the main bacterial genera is available in the SI (Table S1) for growth periods of 1, 14 and 28 days. It is worth noticing that a shift in microbial community composition was observed during this preliminary experiment. Microbial adaptation to the aquatic environment in the pipes might explain the discontinuity of biofilm growth observed at day 14 of the experiment.

Biofilm mobilization phase (flushing)

At the end of the 28 d growth period, the flow rate was set to zero in pipe loops A and B. The pipes were then isolated by closing the valves at the inlet and outlet of the pipe loops. Prior to the start of the flushing phase, the water in the tanks and the auxiliary pipes connected to the main pipe loop were flushed at the maximum flow rate with fresh drinking water from the Kingston network. This was done to mobilize and eliminate the biofilms and other materials that may have accumulated in the tanks and suction/discharge piping at the pumps during the biofilm growth period. The valves at the inlet and outlet of the pipe loops were then re-opened, and the pipes were flushed at an elevated flow rate of 6.5 L s^{-1}

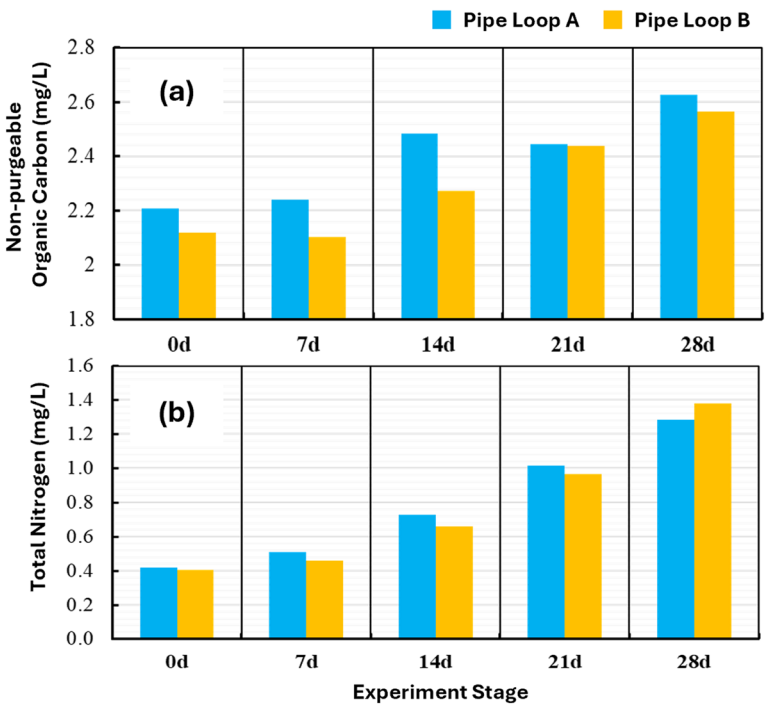

Fig. 2 (a) Non-purgeable organic carbon and (b) total nitrogen established in pipe loops A and B during the 28 d growth phase.

(0.7 m s^{-1}, 1.2 Pa).[57] The water flushed from the pipe loops was sent to a drain and not returned to the tanks. This was done to characterize the mobilization dynamics of the biofilm during flushing. A total of three pipe-loop volumes (5.4 m^3) were flushed through the system.

Sample acquisition during growth and mobilization phases

Bulk water samples. During the biofilm growth phase, bulk water samples were collected weekly, starting with a freshwater sample prior to the IBB inoculation at day 0 and ending at day 28 before flushing. In the flushing phase, a single average bulk water sample was collected at the outlet of the pipe loops. The sample was taken in between the passage of the equivalent pipe loop volume of 25% and 75% during the first pipe loop volume turnover. This sampling campaign was designed to coincide with a period of relative stability during flushing, where the flow rate is fully developed and constant (>25% turnover volume), and not yet diluted with the freshwater front from the tanks (<75% turnover volume).

Bulk water samples were aliquoted and analyzed for several parameters to detect and characterize the presence of bacteria and biofilms in the pipe loops. The bacterial cell concentration (BCC) of the bulk water samples was assessed using a flow cytometer model SH800 from SONY. The samples were fixed with a 5% glutaraldehyde solution, homogenized using high speed vortexing, stained with SYTO BC fluorescent dye that targets DNA of bacterial cells, and counted with the equipment against a standard suspension of reference beads with a known concentration. The rate of bioactivity of the bulk water was assessed using rapid adenosine triphosphate (ATP) tests from Lumina Ultra.

Removable pipe wall samples. In addition to the bulk water samples, removable pipe wall samples were retrieved on a weekly basis from the pipe loops during the experiment. The pipe wall samples consist of round discs cut from identical PVC pipes that are mounted onto the back of the pipe walls of the pipe loops, with a sub-millimeter accuracy of the inner pipe wall surface alignment.[58] Pipe wall samples were collected from three pipe wall sample sections located at the inlet (INL), middle (MID), and outlet (OUT) of the pipe loop and at the invert (INV), springline (SPR), and obvert (OBV) circumferential positions of the pipe (Fig. 1). At the end of every week of the growth phase and immediately after flushing, three pipe wall samples from each longitudinal/circumferential position were retrieved. Each set of three samples were analyzed for i) bacterial cell density (BCD) on the pipe wall, ii) ATP density on the pipe wall, and iii) DNA-labelled fluorescence intensity with a fluorescence microscope. For the bacterial cell density and ATP density, biofilms were retrieved from the pipe wall sample surface using a sterile cotton swab. Subsequently, the swabs were immersed in an aqueous solution, and the biofilm material was resuspended through intense vortexing for 1 minute. Following this, bacterial cell counts and ATP analyses were performed on the biofilm material suspended in solution in a similar manner to those performed on the bulk water samples as previously explained. Specific counting gates in the flow cytometry were calibrated for bulk water and biofilm samples. But the biofilm cell concentration might still have been underestimated due to the presence of undisrupted aggregation of cells.

Fluorescence microscopy. Fluorescence microscopy was used for the *in situ* imaging of the biofilms. First, each pipe wall sample was individually fixed with a 5% glutaraldehyde solution for 15 minutes and stained with a solution of 0.1% TritonX-100 and a SYTO9 fluorescence stain at a concentration of 5 μg L^{-1}. The SYTO 9 fluorophore binds to DNA and affects the fluorescence properties of the DNA molecules that can be visualized using a traditional FITC fluorescence filter cube (excitation at 480 nm and emission at 535 nm), where fluorescence intensity is scaled with DNA concentration. This allows the detection of microorganism cells and EPSs that have extra-cellular DNA embedded in their matrix. After the fixation and staining processes, the samples were washed three times for 1 minute using deionized water.[26] Subsequently, the samples were mounted on an automatic upright fluorescence microscope Nikon Eclipse Ni-E and imaged at a magnification of 100× with a 10× Nikon Plan Fluor Water Dipping objective. A total of 12 fields of view (FOVs) were imaged per sample, using automated imaging software. For each FOV, a *Z*-stack function was used to collect multiple images that spanned a sufficient depth of focus to visualize large biofilm structures (up to a depth of 100 μm), which were later combined into a single focalized image per FOV. Each microscopy sample was processed and imaged individually, and the process was repeated for all 50 samples. Selected FOVs from the images were chosen to highlight the details of the cells and biofilms found on the pipe wall samples during the experiments.

Online monitoring. During the experimental period, several instruments were used to monitor the hydraulic and water quality conditions in the pipe loops. Pressure and flow transducers installed along the pipes were used to measure the flow rate and pressure in the loops. Hach TU5300sc turbidimeters were used to continuously measure turbidity. Sensors were also used to continuously measure the water conductivity, temperature, and dissolved oxygen concentration in the pipe loops. All sensors were set to a sampling frequency of 1 Hz.

Results and discussion

Growth behavior of biofilms at the pipe wall

The first objective of the paper was to examine the biofilm growth behavior at the pipe walls during the growth phase. Fig. 3 indicates a box and whisker plot of the bacterial cell density (BCD) (Fig. 3a) and ATP density (Fig. 3b) measured on the pipe wall samples collected during the experiments from pipe loops A and B. Fig. 3a shows clearly that there was an initial, rapid increase in BCD and ATP in the first 14 days

of the experiment in both pipe loops A and B. This may be owing to the fact that colonizer cells originating from the IBB were migrating from the bulk water to the pipe wall in the early stages of the experiment.[59] Fig. 3a also shows that the increase in BCD was steady but less rapid from day 14 to day 28, and that a maximum value of BCD was reached at day 28 in both pipe loops. The rates of biofilm growth observed here were only possible due to the lack of disinfectants in the system and continuous feed of nutrients.

In pipe loop A, ATP density rose quickly from day 0 to day 14, and then slowly decreased between days 14 and 28 (Fig. 3b). Similarly, in pipe loop B, ATP density rose quickly from day 0 to 14, and then reached a maximum value at day 21, to then see a decrease between days 21 and 28. The median values of BCD and ATP density between pipe loops A and B were different but comparable across the growth and flushing phase. In some instances (*e.g.*, ATP density at day 7), the difference in the data between pipe loops A and B is marked, and might be explained by the fact that patterns of microbial colonization and biofilm growth are seldom uniform in space and in time.[15,26,49] Nevertheless, there was a consistency in the median value and overall trend of the data between pipe loops A and B. This is indicative of the reliability and repeatability of the experimental approach used to harvest and grow drinking water biofilms.

Fig. 4a and b show the time series of (a) bacterial cell concentration (BCC) and (b) intracellular ATP in the bulk water during the 28 d growth period in pipe loops A and B. In this figure, the BCC saw a modest increase between days 0 and 7, a marked increase between days 7 and 14, a small decrease between days 14 and 21, and then a continued increase between days 21 and 28 in pipe loops A and B. The net increase in BCC in the bulk water between days 14 and 28 in Fig. 4a coincided with the slow increase in BCD at the wall (Fig. 3a). The intracellular ATP (Fig. 4b) increased quickly over the first 14 days of the growth period, and then saw a temporary reduction between days 14 and 21, and then continued growth between days 21 and 28. The temporary decrease between days 14 and 21 in both BCC and ATP in the bulk water might be explained by the low concentrations of

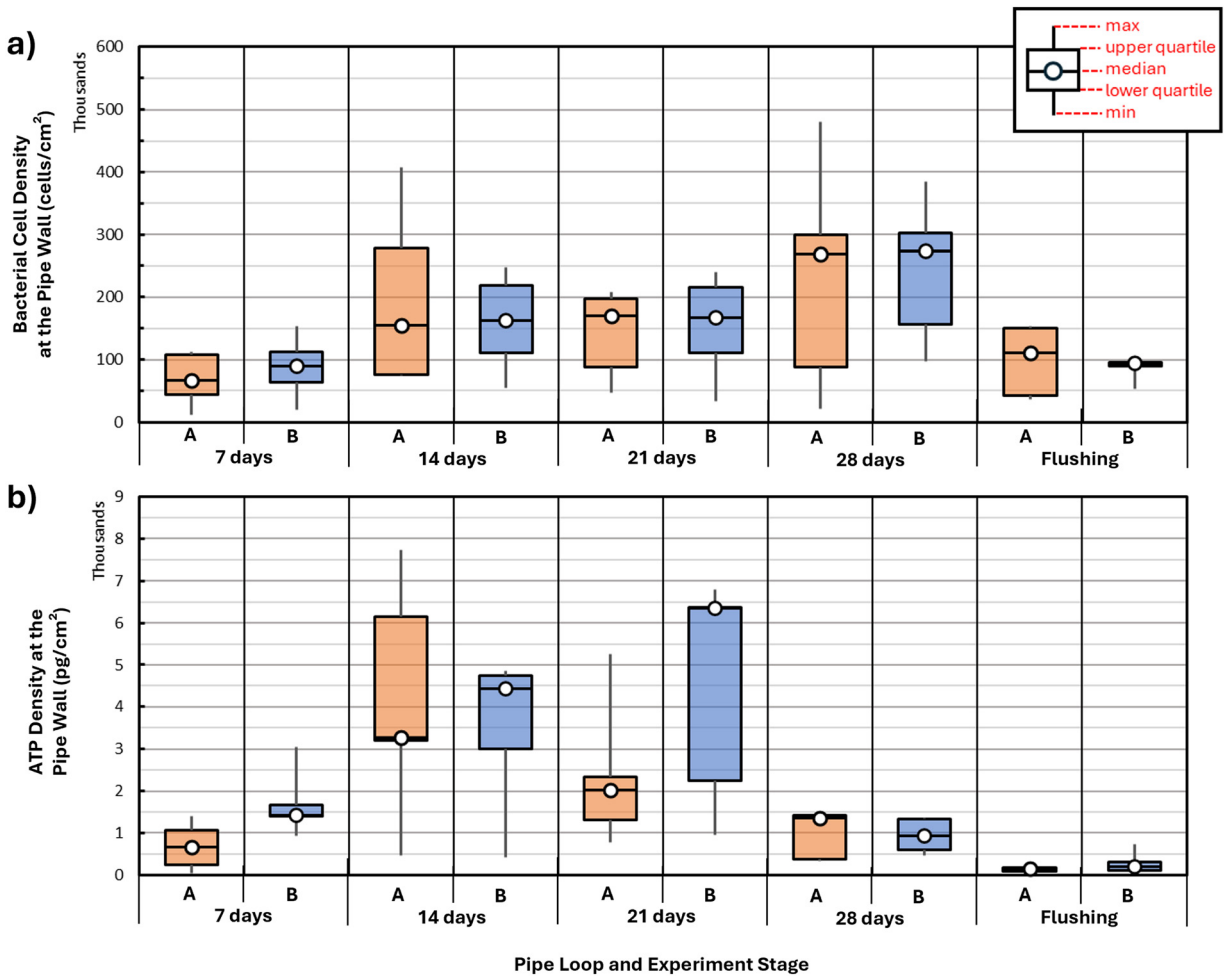

Fig. 3 (a) Bacterial cell density (BCD) and (b) ATP density on the pipe wall samples from both pipe loops A and B during the growth phase and after the flushing phase. Each data point is composed of 5 independent pipe wall sample measurements taken at the five sample positions (INL-INV, MID-INV, MID-SPR, MID-OBV, and OUT-INV). The dashed line and shaded area highlight the average and standard deviation of control samples.

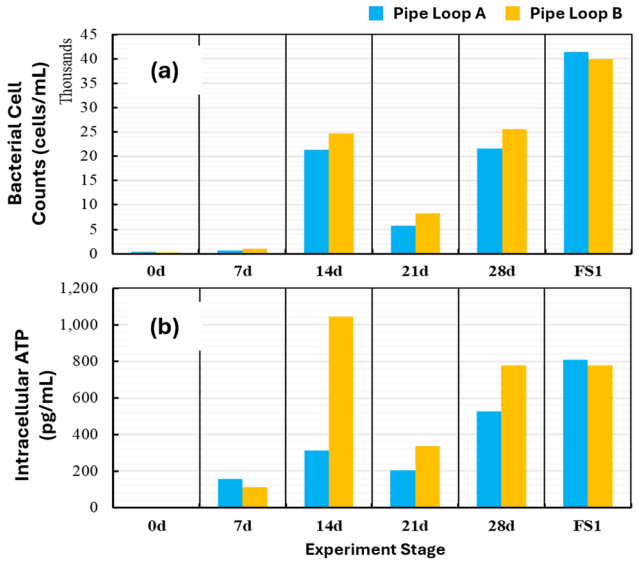

Fig. 4 (a) Bacterial cell counts and (b) intracellular ATP in the bulk water of pipe loops A and B during the 28 d growth phase and after flushing.

DO in the bulk water at that point in the growth stage. The subsequent increase in BCC and ATP between days 21 and 28 might be explained by microbial adaptations and a shift in community composition to adjust to the new DO-limited environment in the bulk water (Fig. S1).

Fluorescence microscopy was also used to make qualitative observations about the biofilm growth behavior at the pipe wall during the growth phase. Fig. 5 shows 40 selected FOVs from 100×-magnified fluorescence images of pipe wall samples, collected at the five locations during the 28 d growth period in pipe loops A and B. The intensity of the green color in the images translates to the concentration of the SYTO9 fluorophore bound to the DNA inside cells and EPSs. The autofluorescence signal of the pipe substrate was not removed with image-processing techniques to highlight the differences between pipe wall samples. Fig. 5 indicates that at day 7, large clusters of biofilms (bright green) were already present at the pipe invert (INV) in the three longitudinal locations. This behavior is consistent with the rapid increase in both BCD and ATP density at the pipe wall previously shown in Fig. 3a and b, which is likely caused by the presence of planktonic clusters of biofilms in the IBB solution inoculated in the pipes. At day 14 in Fig. 5, the SYTO9 intensity was low at the pipe invert in the three longitudinal locations for pipe loops A and B, which suggests that there were fewer cells and EPSs on the wall at this time. This reduction in cells/EPSs at the wall coincided with the marked increase in cell concentration in the bulk water at day 14 in Fig. 4a in both pipe loops. Moreover, Fig. 5 shows the extent to which biofilms (cells/EPSs) increased from days 14 to 28 in both pipe loops. This result agrees with the slow increase in BCD observed at the pipe wall (Fig. 3a) and coincided with the increase in BCC in the bulk water from days 14 through 28 (Fig. 4a).

The findings from Fig. 3 through 5 suggest a plausible storyline of biofilm growth behavior in the pipe loops after their inoculation with the IBB solution. The early-stage biofilms examined in these experiments followed a rapid growth period between days 0 and 14. This early, rapid growth might be attributed to the migration of bacterial colonizers from the bulk water to the pipe wall to initiate biofilm formation. At this point, it is hypothesised that the surface of the pipe wall may have been a more conducive medium for colonizer cells than the bulk water because dissolved nutrients (TN) and carbon levels (NPOC) were not yet high enough to encourage planktonic growth (Fig. 2a and b). During the slower biofilm growth period between days 14 and day 28, the bulk water may have served as a more conducive habitat for cells to grow for several reasons. First, the absence of free chlorine may have encouraged the bacterial population to partition between the bulk water and the pipe wall since these two media could have served as comparably supportive habitats for bacteria. Second, the bacteria in the initial bacterial broth (IBB) introduced into the pipe loop may have been better adapted to a high-nutrient environment. It follows that these bacteria could have favored the bulk water habitat because of the enhanced ability to consume nutrients while living in a planktonic form. Previous research has shown that microorganisms inside biofilms have limited access to food sources because they must rely on the diffusion of dissolved nutrients across small channels and fissures in the biofilm.[60] Third, the bacteria introduced into the pipe loops were likely not well adapted to resisting shear force given that they were grown and harvested on a GAC substrate subjected to low flows and correspondingly low shear forces. Their ability to attach to the pipe wall and remain attached to the wall in the presence of wall shear stress was likely diminished and perhaps partly explains the slow growth of biofilms on the wall. This is supported by previous research which has shown that biofilms conditioned in a low-shear environment have a lower shear strength.[61,62] The fluorescence microscopy data of Fig. 5 also highlighted several important aspects about the structural characteristics of biofilms when attached to the PVC pipe walls. The fluorescence images at the springline (SPR) and obvert (OBV) pipe positions showed a limited number of biofilm clusters throughout the 28 d growth phase. For the most part, the biomass present at the springline and obvert positions was in the form of individual cells adhered to the pipe wall. Biofilms observed at the pipe invert (INV) were found to be held together in large clusters and not uniformly distributed over the pipe area. Biofilm clusters were organized in a manner that small bacterial cells filled the voids between larger cells, and the overall thickness of the clusters was widely variable, ranging from 1–50 μm (vertical distance observed from *Z*-stack microscopy images that enabled focusing of

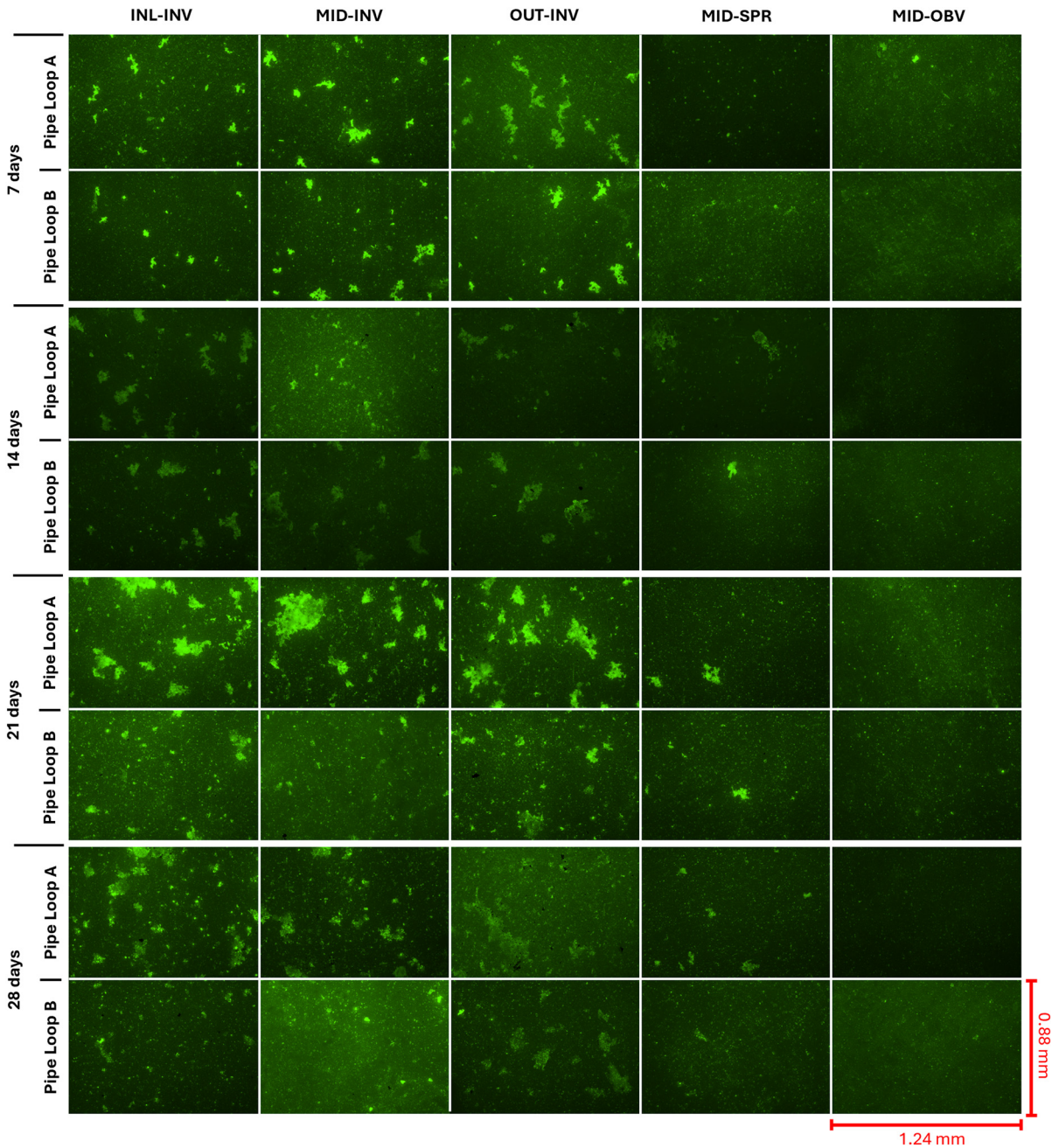

Fig. 5 Selected fields of view from 100× magnified DNA fluorescent-labelled images from pipe wall samples collected for the five pipe wall sample positions: INL-INV located at the pipe loop inlet and invert position, MID-INV located at the pipe loop mid-section and invert position, OUT-INV located at the pipe loop outlet and invert position, MID-SPR located at the pipe loop mid-section and springline position, and MID-OBV located at the pipe loop outlet and obvert position, during the 28 d biofilm growth phase for both pipe loops A and B.

biofilm clusters). Previous research has shown that mature drinking water biofilms typically have a heterogeneous physical structure made up of microcolonies of bacterial cells inside an EPS matrix.[21,60,63] Despite this, the physical structure of biofilms is likely to be environment-specific and depend on many factors such as pipe surface and interface properties, nutrient availability, the microbial community composition of the biofilm, and the hydrodynamic conditions in the pipe.[64] It is unclear if a longer biofilm development period would have led the biofilm clusters observed in the present experiments to expand and fully cover larger pipe areas, or if additional system stressors could have produced biofilms with different structural properties.

The fluorescence images generated from pipe coupon samples taken from pipe loops A and B show the same general trends both in time and in space. The details of each image, such as the specific structure and distribution of the biofilm on the wall, differ between pipe loops A and B. This was expected given the large variability in bacterial

colonization dynamics and the complexity surrounding the evolution of microbial communities inside growing and living biofilms.[15,49]

Biofilm growth behavior in the longitudinal and circumferential locations of the pipe

The analysis was extended to examine the growth behavior of biofilms in the longitudinal and circumferential locations of the pipe loops. In this analysis, bacterial cell density (BCD) was used as a proxy to indicate the presence/absence of biofilms (cells + EPSs). Fig. 6 shows the percent distribution of BCD along the three longitudinal positions (INL, MID, and OUT) at the invert of the pipe (Fig. 6a), and the percent distribution of BCD across the three circumferential positions (INV, SPR, and OBV) at the mid-point location of the pipe loops (Fig. 6b). The results in Fig. 6a suggest that, in general terms, the biofilms were uniformly distributed along the length of the pipe (INL, MID, and OUT) at the invert position. The average percent distribution of cells was 37% at the inlet (INL), 28% at the mid-section (MID), and 36% at the outlet (OUT) across the 28 d growth period for pipe loops A and B. This was qualitatively corroborated by the fluorescence images in Fig. 5. By comparison, Fig. 6b shows that the biofilms were not uniformly distributed across the three circumferential positions (INV, SPR, and OBV) at the mid-section of the pipe loops. On average, 52% of the BCD was found at the pipe invert (INV), 26% of the BCD at the springline (SPR), and 22% of the BCD at the obvert (OBV) across the 28 d growth period for pipe loops A and B. These findings agree with the fluorescence data in Fig. 5 which showed a small number of biofilm clusters in the springline and obvert locations and that most of the biomass found in these circumferential positions was in the form of individual cells. After flushing, the percent distribution of BCD remained largely uniform in the longitudinal direction (Fig. 6a), and non-uniform in the circumferential direction (Fig. 6b). The data in Fig. 6 consistently showed the same trends between pipe loops A and B, even if there were differences in the quantities of percent distribution between the two data sets.

The outcomes of the experiments showed clearly that biofilms predominantly occurred at the invert position of the pipes (Fig. 6b). This was confirmed by the fluorescence microscopy data (Fig. 5) which showed that biofilm clusters were already visible at the invert position after the first week of the experiment. This behavior was unexpected since previous research has indicated that biofilms grow uniformly across the circumference of a pipe.[15,41,49] Instead, biofilms observed in this experiment behaved like large particulate metals (*e.g.*, iron and manganese) found in drinking water that are prone to settling on the invert of pipes.[53,65–67] This might suggest that large clusters of bacteria may have been present in the initial inoculum of the system, and despite their expected lower density in comparison with metal particulates, these clusters still managed to settle to the invert position of the pipes.

Furthermore, the hypothesis that biofilm clusters behave like large particles and settle onto the pipe invert does not

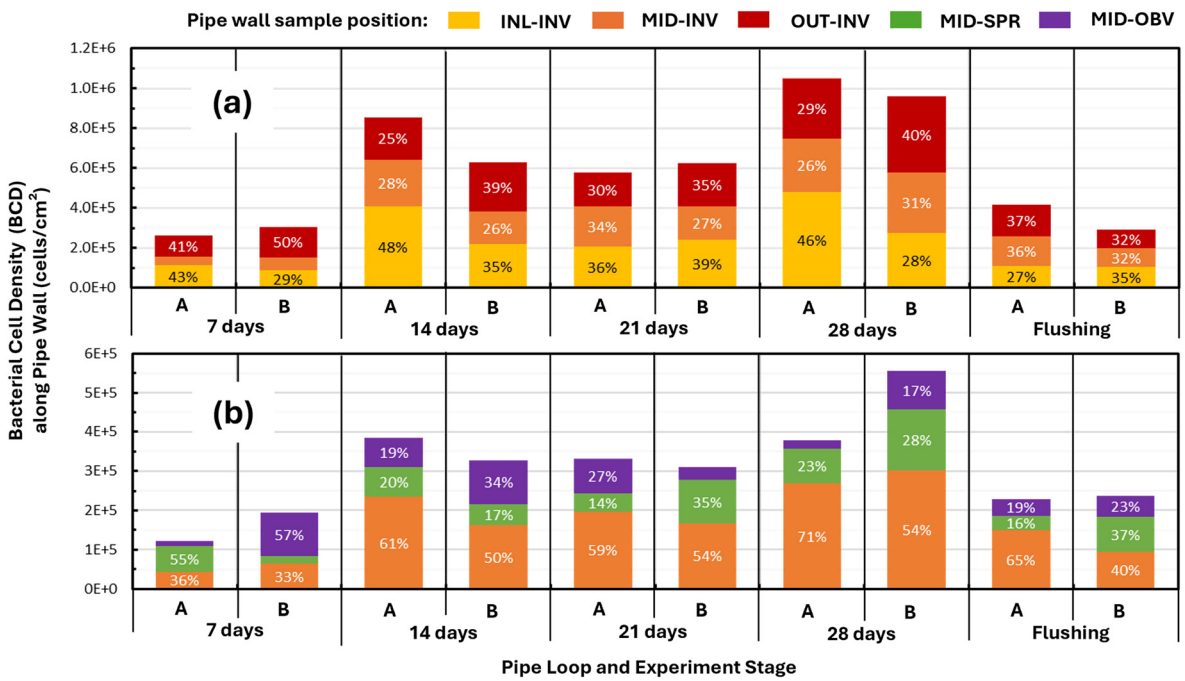

Fig. 6 Percent distribution of bacterial cells on the pipe wall along the (a) longitudinal direction and (b) circumferential position of pipe loops A and B, at different stages of the experiment for the 5 pipe wall sample positions: INL-INV located at the inlet of the loop at the pipe invert, MID-INV located in the mid-section of the loop at the pipe invert, OUT-INV located at the outlet of the loop at the pipe invert, MID-SPR located at the mid-section of the loop at the pipe springline, and MID-OBV located at the mid-section of the loop at the pipe obvert.

explain the absence of new biofilm growth at the springline and obvert pipe positions after the 28 day growth phase. This result was unexpected since there was an abundant quantity of planktonic bacteria in the bulk water to colonize the springline and obvert pipe positions and enough turbulence (Reynolds number of 7000) to drive bacteria to these pipe positions. In this case, the lack of bacterial attachment and biofilm development along the rest of the pipe circumference is largely unexplained. But previous research on biofilms suggested that the presence of environmental stressors can be responsible for triggering microbial mechanisms to form biofilms, such as enhanced cell adhesion to solid surfaces, and EPS production.[6,7] Perhaps the absence of disinfectants and the level of nutrients used in the experiments inhibited the attachment of new bacteria to uncolonized pipe walls. Future experiments with different bacterial loading strategies and system stressors (*e.g.*, low concentrations of disinfectant) are required to further understand the exclusive occurrence of biofilms on the pipe invert position observed here.

Mobilization behavior of biofilms during flushing

The second objective of this paper was to examine the mobilization behavior of the biofilms when subjected to high shear stress during flushing. The results in Fig. 3a and b show that biofilm detachment did occur since both BCD and ATP density at the pipe wall decreased after the pipe loops were flushed at a flow rate of 6.5 L s^{-1} (1.2 Pa). This is corroborated by the results in Fig. 6a and b which showed a corresponding decrease in BCD after flushing at all longitudinal locations and at all circumferential positions in both pipe loops. Fig. 6b shows that while flushing the pipe loops changed the relative proportion of biofilms at the three circumferential positions, most of the remaining biofilm after flushing was located at the pipe invert, just as it was during the growth period. Evidence of biofilm detachment in Fig. 3 and 6 was supported by the bulk water results in Fig. 4a, which showed a 74% increase in BCC (pipe loop B) in the bulk water after flushing. This is further evidence that flushing was able to detach biofilms from the pipe wall and mobilize cells and EPSs into the bulk water.

There is also evidence from the fluorescence microscopy data that biofilms may have been mobilized into the bulk water as flocs or clusters after being detached from the pipe wall during flushing. Fig. 7 shows 12 fields of view of the biofilm on the pipe invert stained with the SYTO9 fluorophore at the inlet (INL), midpoint (MID) and outlet (OUT) locations of the two pipe loops at day 28 and after flushing. The distribution of SYTO9 light intensity in Fig. 7 indicates that after 28 days of growth, the biofilms had a distinct clustering structure. Fig. 7 also shows that, after flushing, there was an increase in the number of biofilm clusters at the midpoint (MID) and outlet (OUT) locations (particularly evident in pipe loop A). This suggests that biofilms may have been transported by the flow from upstream to downstream locations after detachment.

The pipe coupon and bulk water data suggest two items about the biofilm mobilization behavior. First, the wall shear stress of 1.2 Pa imposed during flushing was not sufficient to mobilize all the biofilms from the pipe wall. This finding is

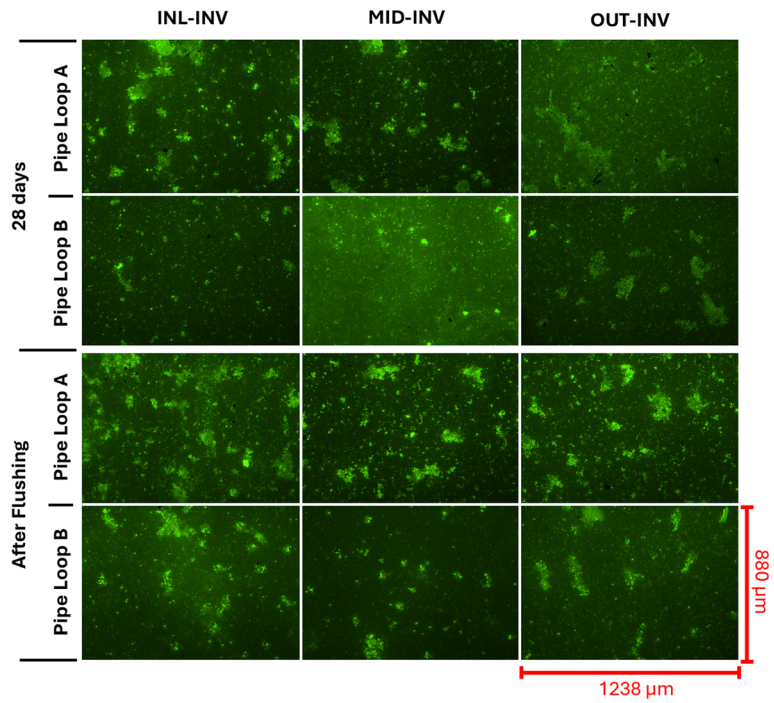

Fig. 7 Fields of view from 100× magnified DNA fluorescent-labelled images from pipe wall samples collected in locations INL-INV, MID-INV, and OUT-INV at day 28 and after flushing in pipe loops A and B.

supported by previous research which found that biofilms remained on the wall even after being subjected to shear stresses almost twice as high as those they experienced during their development and conditioning.[41] Second, biofilms were detached in upstream sections during flushing and transported to downstream sections where they may have settled to the pipe invert at those downstream locations. This hypothesis is supported by fluorescence microscopy data that showed that the majority of biofilms were located at the pipe invert, even after flushing. At this juncture, it is unclear why the biofilms were transported as flocs/clusters by the bulk water and settled as flocs/clusters on the pipe wall. This behavior is akin to the phenomenon of particle mobilization observed in iron oxide particles.[34,53] Further research is needed to understand the causes of clustering in biofilm growth, detachment, and transport in the bulk water.

Limitations

The methods used to examine the growth behavior of biofilms come with some limitations. The authors developed a GAC system to produce the initial bacterial broth (IBB) to inoculate the pipe loop. This GAC system was designed to remove free chlorine from the Kingston water and provide a favorable substrate for bacteria to grow free of any physical stressors (shear) in a nutrient-rich environment. These conditions do not usually exist in drinking water pipes, where disinfectants are present, there is flowing fluid that generates a shear stress at the wall where biofilms are present, and the nutrient environment is typically oligotrophic. This means that the approach used to generate the IBB likely selected for bacteria that were well suited to an unchlorinated, nutrient-rich environment with few physical stressors. It is likely that the bacteria that were able to colonize the pipe wall and live a sessile existence in the biofilm had different microbial community composition and structural properties than those found in actual distribution networks. It is not known at this point to what extent these laboratory conditions contributed to the biofilm clustering observed during the growth and flushing phases.

For practical reasons, the focus of the study was placed on examining the growth of early-stage biofilms under a limited time window of 28 days. In real drinking water systems, biofilms usually grow and mature at a slower rate over a longer period (months and years). This is due to the adverse conditions that exist in a drinking water pipe (presence of a disinfectant, variable shear force at the wall, and a low concentration of nutrients). Previous microbial succession studies have shown that the structural morphology and community composition of early-stage biofilms can differ from mature biofilms with respect to bacterial cell count, EPS levels, bacterial richness, and population stability. For example, in a previous succession study, it was found that mature biofilms (~500 to 1000 days) had a greater cell count, a greater level of bacterial richness, and a more stable population than young biofilms (~1 to 100 days).[68] In the present study, it is unclear how the growth behavior of the biofilms would have evolved had the experiment been extended over a longer period.

The pilot scale laboratory facility used in this study comprises two pipe loops with a PVC pipe material. By contrast, actual drinking water networks have multiple pipe materials (*e.g.*, ductile iron, cast iron, and concrete) of varying ages and conditions. The surface roughness of some of these materials is very different than PVC. This means that, at a microscopic level, the substrate for bacteria to colonize and form biofilms is also different. PVC pipes are smooth and so have relatively small material protrusions and valleys for bacteria to fill and form biofilms.[69] Further, the adhesives, plasticizers, stabilizers in plastic pipes have been found to be a source of nutrients for bacteria.[70] By comparison, iron-based pipes tend to be rougher with more surface features that provide more niches for biofilm adhesion and growth than do plastic pipes.[71] The result is that biofilms in actual distribution systems with different pipe materials may exhibit different structural and adhesive properties compared to those observed in this study.

Conclusions

The aim of this paper was to examine the growth and mobilization behavior of early-stage biofilms in a full-scale, controlled PVC drinking water system. Biofilm growth was assisted by the selection of biofilm-forming microorganisms from local tap water. Each experiment was composed of a 28 d growth phase, where a constant flow rate of 0.6 L s^{-1} (0.07 m s^{-1}, 0.015 Pa) was maintained and nutrients were added to the pipe environment to encourage biofilm growth on the pipe wall. Following the growth period, the flow rate was increased to 6.5 L s^{-1} (0.7 m s^{-1}, 1.2 Pa) to mobilize the biofilms from the pipe wall. The main findings of the paper were: (1) biofilms followed a consistent growth on the pipe wall between 0 and 14 days and 21 to 28 days; (2) biofilm growth was stopped during an apparent transition period between 14 and 21 days, likely because of a shift in bacterial community composition; (3) biofilms were observed at the pipe invert, while few biofilms were detected at the springline and obvert positions. In these circumferential positions, only individual cells adhered to the pipe wall were detected. Biofilms were also observed to be somewhat uniformly distributed along the length of the pipe; (4) flushing flows of 6.5 L s^{-1} (1.2 Pa) could not fully remove the biofilms from the pipe wall; (5) biofilms were observed to form in clusters on the pipe wall that remained fully attached to the pipe wall even after flushing. The characteristics of biofilms achieved in these experiments were likely impacted by the methods used to accelerate microbial activity. Despite that, they were grown from microbes originating from tap water and under similar hydraulic conditions of DWDSs, therefore, partially preserving key biofilm structures of these systems, like their resistance to wall shear stress and mobilization. The research findings add to the emerging knowledge concerning the

growth and mobilization of biofilms in drinking water systems. In addition, the alternative method to investigate biofilms is highly reproducible and can facilitate future studies in the field.

Author contributions

All authors contributed to the contextualization, formal analysis, and methodology of the study. Artur Sass Braga led the data curation and was primarily responsible for writing and revising the manuscript. Yves Filion contributed to the writing process and secured funding for the research. Benjamin Anderson participated equally in the conceptual and analytical aspects of the study.

Conflicts of interest

There are no conflicts to declare.

Abbreviations

DWDS	Drinking water distribution system
DWDL	Drinking water distribution laboratory
EPSs	Extracellular polymeric substances
ATP	Adenosine triphosphate
VSS	Volatile suspended solids
VDS	Volatile dissolved solids
NPOC	Non-purgeable organic carbon
TN	Total nitrogen
BCC	Bacterial cell concentration
BCD	Bacterial cell density
FOV	Field of view

Data availability

All data supporting the findings of this study are included within the manuscript.

Supplementary information is available. See DOI: https://doi.org/10.1039/d5ew00654f.

References

1 H. C. Flemming and J. Wingender, The biofilm matrix, *Nat. Rev. Microbiol.*, 2010, **8**(9), 623–633, DOI: 10.1038/nrmicro2415.
2 C. A. Nkemngong, M. G. Voorn, X. Li, P. J. Teska and H. F. Oliver, A rapid model for developing dry surface biofilms of Staphylococcus aureus and Pseudomonas aeruginosa for in vitro disinfectant efficacy testing, *Antimicrob. Resist. Infect. Control*, 2020, **9**(1), 134, DOI: 10.1186/s13756-020-00792-9.
3 Y. Chao, Y. Mao, Z. Wang and T. Zhang, Diversity and functions of bacterial community in drinking water biofilms revealed by high-throughput sequencing, *Sci. Rep.*, 2015, **5**, 10044, DOI: 10.1038/srep10044.
4 Y. F. Dufrene and A. Persat, Mechanomicrobiology: how bacteria sense and respond to forces, *Nat. Rev. Microbiol.*, 2020, **18**(4), 227–240, DOI: 10.1038/s41579-019-0314-2.
5 M. Krsmanovic, D. Biswas, H. Ali, A. Kumar, R. Ghosh and A. K. Dickerson, Hydrodynamics and surface properties influence biofilm proliferation, *Adv. Colloid Interface Sci.*, 2021, **288**, 102336, DOI: 10.1016/j.cis.2020.102336.
6 H. C. Flemming, J. Wingender, U. Szewzyk, P. Steinberg, S. A. Rice and S. Kjelleberg, Biofilms: an emergent form of bacterial life, *Nat. Rev. Microbiol.*, 2016, **14**(9), 563–575, DOI: 10.1038/nrmicro.2016.94.
7 P. Erdei-Tombor, G. Kiskó and A. Taczman-Brückner, Biofilm Formation in Water Distribution Systems, *Processes*, 2024, **12**(2), 280.
8 B. A. Hemdan, G. E. El-Taweel, P. Goswami, D. Pant and S. Sevda, The role of biofilm in the development and dissemination of ubiquitous pathogens in drinking water distribution systems: an overview of surveillance, outbreaks, and prevention, *World J. Microbiol. Biotechnol.*, 2021, **37**(2), 36, DOI: 10.1007/s11274-021-03008-3.
9 Y. Zhu, H. Wang, X. Li, C. Hu, M. Yang and J. Qu, Characterization of biofilm and corrosion of cast iron pipes in drinking water distribution system with UV/Cl2 disinfection, *Water Res.*, 2014, **60**, 174–181, DOI: 10.1016/j.watres.2014.04.035.
10 G. E. Pizarro and I. T. Vargas, Biocorrosion in drinking water pipes, *Water Supply*, 2016, **16**(4), 881–887, DOI: 10.2166/ws.2016.018.
11 K. C. Makris, S. S. Andra and G. Botsaris, Pipe Scales and Biofilms in Drinking-Water Distribution Systems: Undermining Finished Water Quality, *Crit. Rev. Environ. Sci. Technol.*, 2014, **44**(13), 1477–1523, DOI: 10.1080/10643389.2013.790746.
12 G. Liu, Y. Tao, Y. Zhang, M. Lut, W. J. Knibbe, P. van der Wielen, W. Liu, G. Medema and W. van der Meer, Hotspots for selected metal elements and microbes accumulation and the corresponding water quality deterioration potential in an unchlorinated drinking water distribution system, *Water Res.*, 2017, **124**, 435–445, DOI: 10.1016/j.watres.2017.08.002.
13 H. Armand, I. I. Stoianov and N. J. D. Graham, A holistic assessment of discolouration processes in water distribution networks, *Urban Water J.*, 2015, **14**(3), 263–277, DOI: 10.1080/1573062x.2015.1111912.
14 J. Boxall, I. Douterelo, K. E. Fish and S. Husband, Linking discolouration modelling and biofilm behaviour within drinking water distribution systems, *Water Supply*, 2016, **16**(4), 942–950, DOI: 10.2166/ws.2016.045.
15 I. Douterelo, M. Jackson, C. Solomon and J. Boxall, Spatial and temporal analogies in microbial communities in natural drinking water biofilms, *Sci. Total Environ.*, 2017, **581–582**, 277–288, DOI: 10.1016/j.scitotenv.2016.12.118.
16 I. B. Gomes, M. Simoes and L. C. Simoes, An overview on the reactors to study drinking water biofilms, *Water Res.*, 2014, **62**, 63–87, DOI: 10.1016/j.watres.2014.05.039.
17 I. M. Oliveira, I. B. Gomes, L. C. Simões and M. Simões, A review of research advances on disinfection strategies for biofilm control in drinking water distribution systems, *Water Res.*, 2024, **253**, 121273, DOI: 10.1016/j.watres.2024.121273.

18 M. F. Lemus Pérez and M. Rodríguez Susa, Exopolymeric substances from drinking water biofilms: Dynamics of production and relation with disinfection by products, *Water Res.*, 2017, **116**, 304–315, DOI: 10.1016/j.watres.2017.03.036.
19 D. Zhong, W. Ma, X. Jiang, Y. Yuan, H. Li and Y. Li, Biofilm microbial diversity under conditions of different pipe materials and chlorine residual levels, *Desalin. Water Treat.*, 2018, **133**, 191–198, DOI: 10.5004/dwt.2018.23042.
20 H. Sun, B. Shi, Y. Bai and D. Wang, Bacterial community of biofilms developed under different water supply conditions in a distribution system, *Sci. Total Environ.*, 2014, **472**, 99–107, DOI: 10.1016/j.scitotenv.2013.11.017.
21 H. G. Healy, A. Ehde, A. Bartholow, R. S. Kantor and K. L. Nelson, Responses of drinking water bulk and biofilm microbiota to elevated water age in bench-scale simulated distribution systems, *npj Biofilms Microbiomes*, 2024, **10**(1), 7, DOI: 10.1038/s41522-023-00473-6.
22 L. Mathieu, I. Bertrand, Y. Abe, E. Angel, J. C. Block, S. Skali-Lami and G. Francius, Drinking water biofilm cohesiveness changes under chlorination or hydrodynamic stress, *Water Res.*, 2014, **55**, 175–184, DOI: 10.1016/j.watres.2014.01.054.
23 K. L. G. Learbuch, H. Smidt and P. W. J. J. van der Wielen, Influence of pipe materials on the microbial community in unchlorinated drinking water and biofilm, *Water Res.*, 2021, **194**, 116922, DOI: 10.1016/j.watres.2021.116922.
24 C. Calero Preciado, J. Boxall, V. Soria-Carrasco, S. Martínez and I. Douterelo, Implications of Climate Change: How Does Increased Water Temperature Influence Biofilm and Water Quality of Chlorinated Drinking Water Distribution Systems?, *Front. Microbiol.*, 2021, **12**, DOI: 10.3389/fmicb.2021.658927.
25 I. Douterelo, R. Sharpe and J. Boxall, Bacterial community dynamics during the early stages of biofilm formation in a chlorinated experimental drinking water distribution system: implications for drinking water discolouration, *J. Appl. Microbiol.*, 2014, **117**(1), 286–301, DOI: 10.1111/jam.12516.
26 K. E. Fish, R. Collins, N. H. Green, R. L. Sharpe, I. Douterelo, A. M. Osborn and J. B. Boxall, Characterisation of the physical composition and microbial community structure of biofilms within a model full-scale drinking water distribution system, *PLoS One*, 2015, **10**(2), e0115824, DOI: 10.1371/journal.pone.0115824.
27 F. C. Pick and K. E. Fish, Emerging investigator series: optimisation of drinking water biofilm cell detachment and sample homogenisation methods for rapid quantification via flow cytometry, *Environ. Sci.: Water Res. Technol.*, 2024, **10**(4), 797–813, DOI: 10.1039/D3EW00553D.
28 R. Álvarez-Arroyo, J. I. Pérez, L. M. Ruiz and M. A. Gómez, Chlorination by-products formation in a drinking water distribution system treated by ultrafiltration associated with pre-ozonation or coagulation/flocculation, *J. Water Process Eng.*, 2022, **47**, 102779, DOI: 10.1016/j.jwpe.2022.102779.
29 N. Farhat, L. Kim, K. Mineta, M. Alarawi, T. Gojobori, P. Saikaly and J. Vrouwenvelder, Seawater desalination based drinking water: Microbial characterization during distribution with and without residual chlorine, *Water Res.*, 2022, **210**, 117975, DOI: 10.1016/j.watres.2021.117975.
30 J. Inkinen, B. Jayaprakash, M. Ahonen, T. Pitkänen, R. Mäkinen, A. Pursiainen, J. W. Santo Domingo, H. Salonen, M. Elk and M. M. Keinänen-Toivola, Bacterial community changes in copper and PEX drinking water pipeline biofilms under extra disinfection and magnetic water treatment, *J. Appl. Microbiol.*, 2018, **124**(2), 611–624, DOI: 10.1111/jam.13662.
31 J. Zhang, W. Li, J. Chen, F. Wang, W. Qi and Y. Li, Impact of disinfectant on bacterial antibiotic resistance transfer between biofilm and tap water in a simulated distribution network, *Environ. Pollut.*, 2019, **246**, 131–140, DOI: 10.1016/j.envpol.2018.11.077.
32 C. Jungfer, F. Friedrich, J. Varela Villarreal, K. Brandle, H. J. Gross, U. Obst and T. Schwartz, Drinking water biofilms on copper and stainless steel exhibit specific molecular responses towards different disinfection regimes at waterworks, *Biofouling*, 2013, **29**(8), 891–907, DOI: 10.1080/08927014.2013.813936.
33 M. d. S. P. Agostinho, A. S. Braga, B. Anderson, Y. Fillion and C. V. S. Fernandes, Examining the Effect of Small-Amplitude Transients on the Shear Strength of Biofilms in Water Distribution Pipes, *Eng. Proc.*, 2024, **69**(1), 204.
34 A. S. Braga and Y. Filion, Initial stages of particulate iron oxide attachment on drinking water PVC pipes characterized by turbidity data and brightfield microscopy from a full-scale laboratory, *Environ. Sci.: Water Res. Technol.*, 2022, **8**, 1195–1210, DOI: 10.1039/D2EW00010E.
35 F. Waegenaar, T. Pluym, L. Coene, J. Schelfhout, C. García-Timermans, B. De Gusseme and N. Boon, Impact of temperature and water source on drinking water microbiome during distribution in a pilot-scale study, *npj Clean Water*, 2024, **7**(1), 76, DOI: 10.1038/s41545-024-00371-0.
36 F. Waegenaar, T. Pluym, E. Vermeulen, B. D. Gusseme and N. Boon, Impact of flushing procedures on drinking water biostability and invasion susceptibility in distribution systems, *Appl. Environ. Microbiol.*, 2025, **91**(6), DOI: 10.1128/aem.00686-25.
37 I. Douterelo, K. E. Fish and J. B. Boxall, Succession of bacterial and fungal communities within biofilms of a chlorinated drinking water distribution system, *Water Res.*, 2018, **141**, 74–85, DOI: 10.1016/j.watres.2018.04.058.
38 I. Douterelo, R. L. Sharpe, S. Husband, K. E. Fish and J. B. Boxall, Understanding microbial ecology to improve management of drinking water distribution systems, *Wiley Interdiscip. Rev.: Water*, 2019, **6**(1), e01325, DOI: 10.1002/wat2.1325.
39 D. Quinn, E. Tsagkari, D. S. Bhandari, K. Fish, S. You, W. T. Sloan, J. Boxall and C. J. Smith, Pseudomonas aeruginosa Interactions with Drinking Water Biofilm after an Acute Spike in Annular Bioreactors—Attachment, Persistence, Release, and Reattachment, *Eng. Proc.*, 2024, **69**(1), 148.
40 L. C. Kennedy, S. E. Miller, R. S. Kantor, H. Greenwald, M. J. Adelman, H. Seshan, P. Russell and K. L. Nelson, Stay in the loop: lessons learned about the microbial water quality in

pipe loops transitioned from conventional to direct potable reuse water, *Environ. Sci.: Water Res. Technol.*, 2023, **9**(5), 1436–1454, DOI: 10.1039/D2EW00858K.

41 K. E. Fish and J. B. Boxall, Biofilm Microbiome (Re)Growth Dynamics in Drinking Water Distribution Systems Are Impacted by Chlorine Concentration, *Front. Microbiol.*, 2018, **9**, 2519, DOI: 10.3389/fmicb.2018.02519.

42 Y. Moreno, L. Moreno-Mesonero, P. Soler, A. Zornoza and A. Soriano, Influence of drinking water biofilm microbiome on water quality: Insights from a real-scale distribution system, *Sci. Total Environ.*, 2024, **921**, 171086, DOI: 10.1016/j.scitotenv.2024.171086.

43 J. Huang, S. Chen, X. Ma, P. Yu, P. Zuo, B. Shi, H. Wang and P. J. J. Alvarez, Opportunistic pathogens and their health risk in four full-scale drinking water treatment and distribution systems, *Ecol. Eng.*, 2021, **160**, 106134, DOI: 10.1016/j.ecoleng.2020.106134.

44 J. Boxall, M. Blokker, P. Schaap, V. Speight and S. Husband, Managing discolouration in drinking water distribution systems by integrating understanding of material behaviour, *Water Res.*, 2023, **243**, 120416, DOI: 10.1016/j.watres.2023.120416.

45 J. H. Vreeburg and J. B. Boxall, Discolouration in potable water distribution systems: a review, *Water Res.*, 2007, **41**(3), 519–529, DOI: 10.1016/j.watres.2006.09.028.

46 S. Husband, K. E. Fish, I. Douterelo and J. Boxall, Linking discolouration modelling and biofilm behaviour within drinking water distribution systems, *Water Supply*, 2016, **16**(4), 942–950, DOI: 10.2166/ws.2016.045.

47 N. van Bel, L. M. Hornstra, A. van der Veen and G. Medema, Efficacy of Flushing and Chlorination in Removing Microorganisms from a Pilot Drinking Water Distribution System, *Water*, 2019, **11**(5), 903.

48 Utilities Kingston, *King Street Water Treatment Plant 2023 Annual Report*, Kingston, Ontario, Canada, 2023, https://utilitieskingston.com/Cms_Data/Contents/UtilitiesKingston/Media/Documents/2023-King-Street-Annual-Report-w-Data-fv-240207.pdf.

49 K. Fish, A. M. Osborn and J. B. Boxall, Biofilm structures (EPS and bacterial communities) in drinking water distribution systems are conditioned by hydraulics and influence discolouration, *Sci. Total Environ.*, 2017, **593–594**, 571–580, DOI: 10.1016/j.scitotenv.2017.03.176.

50 S. Liu, C. Gunawan, N. Barraud, S. A. Rice, E. J. Harry and R. Amal, Understanding, Monitoring, and Controlling Biofilm Growth in Drinking Water Distribution Systems, *Environ. Sci. Technol.*, 2016, **50**(17), 8954–8976, DOI: 10.1021/acs.est.6b00835.

51 Y. Abe, S. Skali-Lami, J. C. Block and G. Francius, Cohesiveness and hydrodynamic properties of young drinking water biofilms, *Water Res.*, 2012, **46**(4), 1155–1166, DOI: 10.1016/j.watres.2011.12.013.

52 A. J. Pinto, C. Xi and L. Raskin, Bacterial Community Structure in the Drinking Water Microbiome Is Governed by Filtration Processes, *Environ. Sci. Technol.*, 2012, **46**(16), 8851–8859, DOI: 10.1021/es302042t.

53 A. S. Braga and Y. Filion, The interplay of suspended sediment concentration, particle size and fluid velocity on the rapid deposition of suspended iron oxide particles in PVC drinking water pipes, *Water Res.: X*, 2022, **15**, 100143, DOI: 10.1016/j.wroa.2022.100143.

54 A. Aisopou, I. Stoianov and N. Graham, Modelling Discolouration in WDS Caused by Hydraulic Transient Events, in *Water Distribution Systems Analysis*, 2010, vol. 2011, pp. 522–534.

55 P. S. Husband, J. B. Boxall and A. J. Saul, Laboratory studies investigating the processes leading to discolouration in water distribution networks, *Water Res.*, 2008, **42**(16), 4309–4318, DOI: 10.1016/j.watres.2008.07.026.

56 R. L. Sharpe, C. J. Smith, J. B. Boxall and C. A. Biggs, Pilot Scale Laboratory Investigations into the Impact of Steady State Conditioning Flow on Potable Water Discolouration, in *Water Distribution Systems Analysis*, 2010, vol. 2011, pp. 494–506.

57 A. Sass Braga and Y. Filion, Examining the conditioning factors that influence material shear strength of particle deposits in a full-scale drinking water distribution laboratory, *Environ. Sci.: Water Res. Technol.*, 2023, **9**(10), 2619–2630, DOI: 10.1039/D3EW00159H.

58 A. S. Braga and Y. Filion, A novel monitoring scheme to detect iron oxide particle deposits on the internal surface of PVC drinking water pipes, *Environ. Sci.: Water Res. Technol.*, 2021, **7**(11), 2116–2128, DOI: 10.1039/D1EW00614B.

59 C. Margot, W. Rhoads, M. Gabrielli, M. Olive and F. Hammes, Dynamics of drinking water biofilm formation associated with Legionella spp, colonization, *npj Biofilms Microbiomes*, 2024, **10**(1), 101, DOI: 10.1038/s41522-024-00573-x.

60 R. M. Donlan and J. W. Costerton, Biofilms: Survival Mechanisms of Clinically Relevant Microorganisms, *Clin. Microbiol. Rev.*, 2002, **15**(2), 167–193, DOI: 10.1128/cmr.15.2.167-193.2002.

61 E. Paul, J. C. Ochoa, Y. Pechaud, Y. Liu and A. Line, Effect of shear stress and growth conditions on detachment and physical properties of biofilms, *Water Res.*, 2012, **46**(17), 5499–5508, DOI: 10.1016/j.watres.2012.07.029.

62 C. Wang, L. Miao, J. Hou, P. Wang, J. Qian and S. Dai, The effect of flow velocity on the distribution and composition of extracellular polymeric substances in biofilms and the detachment mechanism of biofilms, *Water Sci. Technol.*, 2013, **69**(4), 825–832, DOI: 10.2166/wst.2013.785.

63 Z. Lewandowski, Structure and Function of Biofilms, in *Biofilms: Recent Advances in Their Study and Control*, ed. L. V. Evans, CRC Press, 2000, pp. 1–17.

64 T. Tolker-Nielsen and S. Molin, Spatial Organization of Microbial Biofilm Communities, *Microb. Ecol.*, 2000, **40**(2), 75–84, DOI: 10.1007/s002480000057.

65 A. Mussared, R. Fabris, J. Vreeburg, J. Jelbart and M. Drikas, The origin and risks associated with loose deposits in a drinking water distribution system, *Water Supply*, 2019, **19**(1), 291–302, DOI: 10.2166/ws.2018.073.

66 J. H. Vreeburg, Discolouration in drinking water systems: a particular approach, *PhD Thesis*, Delft University of Technology, 2007.

67 J. H. Vreeburg, D. Schippers, J. Q. Verberk and J. C. van Dijk, Impact of particles on sediment accumulation in a drinking water distribution system, *Water Res.*, 2008, **42**(16), 4233–4242, DOI: 10.1016/j.watres.2008.05.024.

68 A. C. Martiny, T. M. Jørgensen, H.-J. Albrechtsen, E. Arvin and S. Molin, Long-Term Succession of Structure and Diversity of a Biofilm Formed in a Model Drinking Water Distribution System, *Appl. Environ. Microbiol.*, 2003, **69**(11), 6899–6907, DOI: 10.1128/AEM.69.11.6899-6907.2003.

69 M. W. Cowle, G. Webster, A. O. Babatunde, B. N. Bockelmann-Evans and A. J. Weightman, Impact of flow hydrodynamics and pipe material properties on biofilm development within drinking water systems, *Environ. Technol.*, 2020, **41**(28), 3732–3744, DOI: 10.1080/09593330.2019.1619844.

70 I. Biedroń, T. Traczewska, T. Konieczny and G. Płaza, Characterization of biofilms from selected synthetic materials used in water distribution system, *J. Ecol. Eng.*, 2017, **18**(1), 284–293, DOI: 10.12911/22998993/67850.

71 X. Zhang, T. Lin, F. Jiang, X. Zhang, S. Wang and S. Zhang, Impact of pipe material and chlorination on the biofilm structure and microbial communities, *Chemosphere*, 2022, **289**, 133218, DOI: 10.1016/j.chemosphere.2021.133218.

